ELSEVIER

Comput. Methods Appl. Mech. Engrg. 117 (1994) 71–90

Computer methods in applied mechanics and engineering

A spectral algorithm for the Stokes problem in vorticity–vector potential formulation and cylindrical geometry

R. Pasquetti*, R. Bwemba

Lab. J.A. Dieudonné, URA CNRS 168, Université de Nice-Sophia Antipolis, Parc Valrose, 06108 Nice cedex 2, France

Received 19 January 1993

Abstract

In the numerical computation of incompressible flows using the Navier–Stokes equations, the main task generally lies in the solution of a Stokes type problem. In this paper, we focus on this key point, when using (i) a spectral method, (ii) the vorticity–vector potential formulation of the 3D Navier–Stokes equations and (iii) a cylindrical geometry. At the end we conclude with a numerical test of our Stokes solver in the framework of Rayleigh–Bénard natural convection.

1. Introduction

For incompressible three-dimensional flows, it is well known that the classical velocity–pressure formulation of the Navier–Stokes equations involves difficult problems for the treatment of the pressure and continuity equation, specially when using spectral methods. Although a number of efficient procedures have been suggested to overcome these problems, it is also possible to use other approaches and among them the one based on the vorticity–vector potential formulation. This formulation, which is now well understood from the theoretical point of view [1–5], is a continuation in 3D of the classical vorticity–stream function formulation widely used in 2D problems.

The main task in the solution of the stationary or transient Navier–Stokes equations generally lies in the solution of a stokes type problem. In this paper, our purpose is to focus on this key point, specially when multiple resolutions are needed, i.e. when considering the transient Navier–Stokes equations. In Section 2 we introduce the Stokes problem for confined and simply connected geometries when using the vorticity–vector potential formulation.

In order to get high precision in the calculations, the numerical method used in this work is of spectral type. The geometry under consideration is cylindrical, i.e. simple enough to use such methods, but nevertheless more complicated than the usual Cartesian geometries. The advantage of the cylindrical geometry (ρ, θ, ζ) is clearly that the natural 2π-periodicity along the polar angle θ can be used in a very efficient way; the Fourier analysis permits the substitution of a set of 2D complex problems in the (ρ, ζ) planes to the initial 3D; these 2D problems are then solved by using Chebyshev polynomials. The drawbacks come from the cylindrical coordinate system, for which the operators are more complicated and pseudo-singular and for which it is necessary to ensure some conditions of regularity at the axis. In Section 3 (and Appendix A), we describe the basic step which consists of the resolution of the Helmholtz vectorial equation, when using a Fourier–Chebyshev spectral method.

A major difficulty of the Stokes problem, in the vorticity–vector potential formulation, comes from

* Corresponding author.

SSDI 0045-7825(93)E0229-2

the boundary conditions. For a set of six scalar equations, which correspond to the components of the vorticity and vector potential, we have five boundary conditions for the vector potential and only one for the vorticity vector. Moreover, among these conditions, some are not simply of Dirichlet or Neumann type, or combinations of such boundary conditions. So, in order to obtain the standard situation of two vectorial Helmholtz equations with classical boundary conditions, for both equations we utilize an influence matrix technique which permits the substitution of Dirichlet boundary conditions for those difficult to handle. A difficult point here is that the influence matrices can be singular in multi-dimensional geometries. This part of our algorithm is described in Section 4.

In order to check our Stokes solver in a realistic framework, we use a numerical experiment of Rayleigh–Benard natural convection; the solution of a Stokes problem, the force term of which includes the non-linear convective term and the buoyancy term, is thus needed at each time-step. Such a numerical experiment points out some drawbacks that we essentially attribute to the differences between the properties of the continuous and discrete spectral operators that appear in the governing equations. To overcome these difficulties we complete our resolutions algorithm with an additive step, the 'vorticity correction step', which gives an efficient numerical solution as shown in Section 5.

2. Stokes problem in vorticity–vector potential formulation

The computations of various problems of fluid dynamics, in both stationary or transient cases, need the numerical solution of a Stokes type problem. Considering a confined domain Ω of boundary Γ, in vorticity–vector potential formulation it consists of the determination of the vectors ω and ψ such that in Ω,

$$\nabla^2\omega - \sigma\omega = w\,, \tag{1}$$

$$\nabla^2\psi + \omega = 0\,, \tag{2}$$

with appropriate boundary conditions on Γ. Eq. (1) derives from the vorticity transport equation, which is obtained by taking the curl of the momentum equation. The vector w is thus a divergence-free force term, i.e. $\nabla\cdot w = 0$, which is problem dependent. It can include the non-linear convective term of the vorticity transport equation, some terms calculated at previous time steps for transient problems as well as terms already known, e.g. by solving at first a coupled equation such as the energy equation. The $\sigma\omega$ term appears in transient problems and the coefficient σ (>0) is then associated with the finite difference approximation of the time derivative. The vector ω is the vorticity that we define from the velocity field v by

$$\omega = \nabla\times v\,. \tag{3}$$

The vector potential ψ, assumed to be divergence free, i.e. $\nabla\cdot\psi = 0$, is such that

$$v = \nabla\times\psi\,. \tag{4}$$

By taking the curl of Eq. (4) and then using the well known vectorial relation,

$$\nabla\times\nabla\times\psi = \nabla(\nabla\cdot\psi) - \nabla^2\psi\,, \tag{5}$$

one obtains the Poisson equation (2).

The basic interest of the vorticity–vector potential formulation is that from Eq. (4) the resulting velocity field v automatically satisfies the continuity equation $\nabla\cdot v = 0$. Nevertheless, the vorticity–vector potential formulation exhibits six unknowns (the components of the ω and ψ vectors) instead of four in the velocity–pressure formulation (the components of v and the pressure). This remark is probably the main reason for the rare employment of the formulation, but the major implication is the non-uniqueness of the vector ψ and consequently the possibility of various boundary conditions for this vectorial field.

The boundary conditions which have to be imposed on ω and ψ derive partially from those imposed

on the velocity; in a confined geometry, when assuming Dirichlet boundary conditions, they are written as

$$v_n|_\Gamma = 0\,, \tag{6}$$

$$v_t|_\Gamma = \tilde{v}_t\,, \tag{7}$$

where the subscripts n and t refer to the normal and tangential components of the velocity v and where $\tilde{v}_t$ is given.

Concerning the vector potential ψ, for the confined and simply connected geometries considered in this paper, both theoricians and numericians consider that the following boundary conditions are well suited [1–4]:

$$\psi_t|_\Gamma = 0\,, \tag{8}$$

$$\nabla\cdot\psi|_\Gamma = 0\,, \tag{9}$$

where the vector ψ_t is the projection of ψ on the tangential plane to Γ. Condition (8) implies that the normal velocity is zero, as required by Eq. (6), and condition (9) that ψ is divergence free if ω is divergence free (as shown below). Now, from Eq. (7) one has the additive vectorial boundary condition

$$(\nabla\times\psi)_t|_\Gamma = \tilde{v}_t\,. \tag{10}$$

Concerning the vorticity ω, the boundary conditions for the velocity only imply the scalar boundary condition (from Eq. (7)):

$$\omega_n|_\Gamma = \nabla\times\tilde{v}_t\,. \tag{11}$$

Consequently the vorticity–vector potential formulation of the Stokes problem exhibits only the boundary condition (11) for ω and five conditions for ψ: the scalar condition (9) and the two vectorial (8) and (10) (each one equivalent to two scalar).

It may be surprising that from the boundary condition (7), equivalent to two scalar conditions, one can deduce (10) and (11) which stand for three scalar conditions; thus, a lot of papers criticize the use of (11) and suggest using (see e.g. [6, 7])

$$\nabla\cdot\omega|_\Gamma = 0\,. \tag{12}$$

Nevertheless, when assuming sufficient regularity properties, one can easily demonstrate that the boundary conditions (11) and (12) are equivalent, in the sense that when associating them with the conditions (8), (9) and (10), the solution of the Stokes problem (1), (2) is, as required, such that

$$\omega = \nabla\times\nabla\times\psi\,. \tag{13}$$

(a) Stokes problem (1), (2) with boundary conditions (8), (9), (10) and (12): Taking the divergence of both members of (1) and using the commutativity property of the operators divergence and Laplacian, we have

$$\Delta(\nabla\cdot\omega) - \sigma\nabla\cdot\omega = 0\,, \tag{14}$$

where Δ is the scalar Laplacian operator. This homogeneous scalar Helmholtz equation with the homogeneous boundary condition (12) has for unique solution $\nabla\cdot\omega = 0$. Then, by taking the divergence of (2), one obtains in the same way

$$\Delta(\nabla\cdot\psi) + \nabla\cdot\omega = 0\,. \tag{15}$$

This Laplace equation (since $\nabla\cdot\omega = 0$) with the homogeneous boundary condition (9) has for unique solution $\nabla\cdot\psi = 0$. By eliminating $\nabla^2\psi$ from (5) and (2) and knowing that if $\nabla\cdot\psi = 0$, then $\nabla(\nabla\cdot\psi) = 0$, one obtains the desired result (13).

(b) Stokes problem (1), (2) with boundary conditions (8), (9), (10) and (11): Taking (2) into account, Eq. (5) can be written as

$$\nabla(\nabla\cdot\psi)-\nabla\times\nabla\times\psi+\omega=0\,. \tag{16}$$

Along Γ this vectorial equation can be projected on the unitary normal vector n to the boundary; with the condition (10) we have

$$\partial_n(\nabla\cdot\psi)-(\nabla\times\tilde{v}_t)_n+\omega_n|_\Gamma=0 \tag{17}$$

and from the condition (11),

$$\partial_n(\nabla\cdot\psi)|_\Gamma=0\,. \tag{18}$$

Eqs. (14) and (15), associated with the boundary conditions (9) and (18), constitute a homogeneous scalar Stokes problem for which it is well known that the only solution is $\nabla\cdot\omega=0$ and $\nabla\cdot\psi=0$. As in (a), one can now obtain the desired result (13) from Eqs. (2) and (5).

In the discrete framework, the previous demonstrations are generally no longer valid, because of the loss of the commutativity property of the divergence and Laplacian operators. This is the case with spectral methods, for which it seems that the desired result (13) can only be obtained in an approximative way from the Stokes problem (1), (2). Our numerical experiments have led us to choose the 'classical' boundary condition (12) instead of (11), because (11) implies some specific problems when using the influence matrix technique.

For simplification, the no-slip boundary condition will now be assumed. Thus, the Stokes problem which is considered in the following is written as

$$\nabla^2\omega-\sigma\omega=w\,, \tag{1'}$$

$$\nabla^2\psi+\omega=0\,, \tag{2'}$$

$$\nabla\cdot\omega|_\Gamma=0\,,\qquad \nabla\cdot\psi|_\Gamma=0\,,\qquad \psi_t|_\Gamma=0\,,\qquad (\nabla\times\psi)_t|_\Gamma=0\,, \tag{19}$$

where the vector w is solenoidal ($\nabla\cdot w=0$).

3. Spectral solution of the vectorial Helmholtz type equation in cylindrical coordinates

In Cartesian coordinates, the vectorial Helmholtz equation splits into three scalar Helmholtz equations which can be solved using the standard procedures of the tau or collocation spectral method [8]. On the contrary, the cylindrical coordinate system (ρ,θ,ζ) induces the following drawbacks:

- the Laplacian operator exhibits a pseudosingularity at the axis,
- the vectorial Laplacian is not diagonal, in the sense that a coupling occurs between its first two components,
- some conditions of regularity must be forced at the axis.

In this section it is shown how to solve the vectorial Helmholtz equation when using a pseudospectral method. To this aim, in the Stokes problem (1), (2), (19), we consider Eq. (1), for ω. Temporarly, we make no assumptions concerning the boundary conditions to be associated with this vectorial Helmholtz equation, but this point is discussed at the end of this section.

The difficulty comes at first from the ∇^2 operator which is not diagonal:

$$\nabla^2\omega=\left[\left(\Delta-\frac{1}{\rho^2}\right)\omega_1-\frac{2}{\rho^2}\,\partial_\theta\omega_2\right]e_1+\left[\left(\Delta-\frac{1}{\rho^2}\right)\omega_2+\frac{2}{\rho^2}\,\partial_\theta\omega_1\right]e_2+\Delta\omega_3\,e_3\,, \tag{20}$$

with

$$\Delta=\partial_{\rho\rho}+\frac{1}{\rho}\,\partial_\rho+\frac{1}{\rho^2}\,\partial_{\theta\theta}+\partial_{\zeta\zeta}$$

and where ω_1, ω_2 and ω_3 are the ρ, θ and ζ-components in the cylindrical basis (e_1,e_2,e_3). An efficient way to diagonalize ∇^2 is the transformation [9]:

$$\omega_+=\omega_1+\mathrm{i}\omega_2\,,\qquad \omega_-=\omega_1-\mathrm{i}\omega_2\quad(\mathrm{i}^2=-1) \tag{21}$$

so that in the basis (e_+, e_-, e_3),

$$\nabla^2\omega = \left[\left(\Delta - \frac{1}{\rho^2} + \frac{2\mathrm{i}}{\rho^2}\partial_\theta\right)\omega_+\right]e_+ + \left[\left(\Delta - \frac{1}{\rho^2} - \frac{2\mathrm{i}}{\rho^2}\partial_\theta\right)\omega_-\right]e_- + \Delta\omega_3 e_3 . \tag{22}$$

The complex form of this operator is not a source of difficulty, since in the Fourier analysis that the natural periodicity in θ induces us to use, the operator ∂_θ is simply equal to $\mathrm{i}k$ (k is the mode number); specifying with a '$\wedge$' the variables in Fourier space, one obtains

$$\widehat{\nabla^2\omega} = [\Delta_k^+ \hat{\omega}_+]e_+ + [\Delta_k^- \hat{\omega}_-]e_- + [\Delta_k \hat{\omega}_3]e_3 , \tag{23}$$

where

$$\begin{bmatrix}\Delta_k^+\\ \Delta_k^-\\ \Delta_k\end{bmatrix} = \partial_{\rho\rho} + \frac{1}{\rho}\partial_\rho + \partial_{\zeta\zeta} - \frac{1}{\rho^2}\begin{bmatrix}(k+1)^2\\ (k-1)^2\\ k^2\end{bmatrix} .$$

Then, from the 3D Helmholtz equation (1) one obtains in Fourier spectral space the set of 2D complex uncoupled equations:

$$(\Delta_k^+ - \sigma)\hat{\omega}_+(\rho, \zeta; k) = \hat{w}_+(\rho, \zeta; k) , \tag{24}$$

$$(\Delta_k^- - \sigma)\hat{\omega}_-(\rho, \zeta; k) = \hat{w}_-(\rho, \zeta; k) , \quad 0 \leq k \leq K \ (K \text{ is the number of modes}) . \tag{25}$$

$$(\Delta_k - \sigma)\hat{\omega}_3(\rho, \zeta; k) = \hat{w}_3(\rho, \zeta; k) , \tag{26}$$

To go further in the analysis, we have to define precisely the geometrical support of the different variables. The natural approach is to assume $0 \leq \rho \leq R$ (R is the cylinder radius) and $0 \leq \theta \leq 2\pi$, but the default in this case is (i) the non-natural necessity in the Fourier spectral space of a boundary condition at the ζ axis (see e.g. [10]), and (ii) the difficulty of forcing satisfying properties of regularity at $\rho = 0$. A most suitable approach is to assume $-R \leq \rho \leq R$ and $0 \leq \theta \leq 2\pi$, but in this case some constraints of coherency must be considered; in physical space they are written as

$$\omega_\mu(\rho, \theta, \zeta) = -\omega_\mu(-\rho, \theta + \pi, \zeta) , \quad \mu = 1, 2 , \qquad \omega_3(\rho, \theta, \zeta) = \omega_3(-\rho, \theta + \pi, \zeta) \tag{27}$$

which with straightforward induction in Fourier spectral space, gives

$$\hat{\omega}_\mu(\rho, \zeta; k) = (-1)^{k+1}\hat{\omega}_\mu(-\rho, \zeta; k) , \quad \mu = 1, 2 , \qquad \hat{\omega}_3(\rho, \zeta; k) = (-1)^k\hat{\omega}_3(-\rho, \zeta; k) . \tag{28}$$

Moreover, some properties of regularity are needed at the axis, specially the uniqueness of ω for $\rho = 0$. The uniqueness property obviously requires ω_3 to be independent on the polar angle and for ω_1 and ω_2 to exhibit a sinusoidal variation; in Fourier spectral space, one obtains

$$\hat{\omega}_\mu(\rho = 0, \zeta; k \neq 1) = 0 , \quad \mu = 1, 2 , \qquad \hat{\omega}_3(\rho = 0, \zeta; k \neq 0) = 0 . \tag{29}$$

More generally, to be physical a variable must be infinitely differentiable; in Fourier spectral space and in the (e_+, e_-, e_3) basis, which is a good framework for this study of regularity, one can show that the constraint of analyticity at the axis can be written as

$$\hat{\omega}_+(\rho, \zeta; k) = \rho^{k+1}\tilde{\omega}_+(\rho, \zeta; k) , \qquad \hat{\omega}_-(\rho, \zeta; k) = \rho^{|k-1|}\tilde{\omega}_-(\rho, \zeta; k) ,$$
$$\hat{\omega}_3(\rho, \zeta; k) = \rho^k\tilde{\omega}_3(\rho, \zeta; k) , \tag{30}$$

where the function $\tilde{\omega}_+$, $\tilde{\omega}_-$ and $\tilde{\omega}_3$ are even in ρ and finite at $\rho = 0$. Taking (21) into account, the constraints of uniqueness (29) are clearly included in the constraints of regularity (30). Constraints (30) can be demonstrated [11, 12], by using in Fourier spectral space the standard polynomial basis $\rho^i\zeta^j$, i, $j \geq 0$, and imposing $\nabla^{2l}\omega$ to be not singular at $\rho = 0$ for $l \geq 0$.

In order to take into account the constraints of analyticity, the natural idea is to use the changes of variables defined by (30) and to solve in $\tilde{\omega}_+$, $\tilde{\omega}_-$ and $\tilde{\omega}_3$ rather than in $\hat{\omega}_+$, $\hat{\omega}_-$ and $\hat{\omega}_3$. But numerical

difficulties arise for high values of the mode number k. That is the reason why we suggest the following algorithm which forces the ρ exponent to be smaller or equal to an integer M:

$$\hat{\omega}_+(\rho,\zeta;k)=\rho^{m+1}\tilde{\omega}_+(\rho,\zeta;k)\,,\qquad \hat{\omega}_-(\rho,\zeta;k)=\rho^{|m-1|}\tilde{\omega}_-(\rho,\zeta;k)\,,$$
$$\hat{\omega}_3(\rho,\zeta;k)=\rho^{m}\tilde{\omega}_3(\rho,\zeta;k)\,, \tag{31}$$

with

$$\begin{aligned} &m+\varepsilon=k+\varepsilon,\ \varepsilon=\{1,-1,0\}\,, && \text{if } k+\varepsilon\leq M\,,\\ &m+\varepsilon=M\,, && \text{if } k+\varepsilon>M,\ k+\varepsilon \text{ and } M \text{ of same parity}\,,\\ &m+\varepsilon=M-1\,, && \text{if } k+\varepsilon>M,\ k+\varepsilon \text{ and } M \text{ of inverse parity}\,. \end{aligned}$$

Such an algorithm only imposes $\nabla^{2l}\omega$, $0\leq l\leq (M-1)/2$, to be not singular; one can note that the weaker condition, which requires that all the usual operators are not singular, is obtained for M equal to 3. Let us mention that in spherical geometry, an approach similar to ours can be found in [13]. After the change of variables (31), one obtains the set of equations

$$(\Delta^{+}_{k,m}-\sigma)\tilde{\omega}_+(\rho,\zeta;k)=\tilde{w}_+(\rho,\zeta;k)\,, \tag{32}$$

$$(\Delta^{-}_{k,m}-\sigma)\tilde{\omega}_-(\rho,\zeta;k)=\tilde{w}_-(\rho,\zeta;k)\,,\quad 0\leq k\leq K\,, \tag{33}$$

$$(\Delta_{k,m}-\sigma)\tilde{\omega}_3(\rho,\zeta;k)=\tilde{w}_3(\rho,\zeta;k)\,, \tag{34}$$

with

$$\begin{bmatrix}\Delta^{+}_{k,m}\\ \Delta^{-}_{k,m}\\ \Delta_{k,m}\end{bmatrix}=\partial_{\rho\rho}+\frac{1}{\rho}\begin{bmatrix}2m+3\\ 2|m-1|+1\\ 2m+1\end{bmatrix}\partial_{\rho}+\partial_{\zeta\zeta}-\frac{1}{\rho^2}\begin{bmatrix}(k+1)^2-(m+1)^2\\ (k-1)^2-(m-1)^2\\ k^2-m^2\end{bmatrix}$$

and where $\tilde{w}_+$, $\tilde{w}_-$ and $\tilde{w}_3$ are the corresponding values of $\hat{w}_+$, $\hat{w}_-$ and $\hat{w}_3$, by transformations (31).

Eqs. (32)–(34) form a set of uncoupled 2D complex equations that we solve by using a Chebyshev–Chebyshev collocation method. In Appendix A we describe this technical part of the work, by focusing on the governing equation (34) of the $\tilde{\omega}_3$ component.

Now, let us come back to the boundary conditions which can be associated with the vectorial Helmholtz equation, when following the approach described in this section.

A large class of linear boundary conditions can be supported for the ζ-component; They may read

$$(\alpha_3\omega_3+\beta_3\,\partial_{\mathrm{n}}\omega_3)|_{\Gamma}=f_3\,, \tag{35}$$

where ∂_{n} is the normal derivative operator, f_3 a space dependent function defined on Γ and where α_3 and β_3 are parameters that do not depend on the polar angle θ, in order to permit the Fourier analysis. In Appendix A, due to the use of the Chebyschev–Chebyschev collocation method, these coefficients are also supposed constant on each part of the cylinder surface.

For the ρ and θ components, it can be easily observed that the boundary conditions must be of the same kind; they may read

$$\begin{aligned}&(\alpha_{\pm}\omega_1+\beta_{\pm}\,\partial_{\mathrm{n}}\omega_1)|_{\Gamma}=f_1\,,\\ &(\alpha_{\pm}\omega_2+\beta_{\pm}\,\partial_{\mathrm{n}}\omega_2)|_{\Gamma}=f_2\,,\end{aligned} \tag{36}$$

where f_1 and f_2 are space dependent functions defined on Γ and where $\alpha_{\pm}$ and $\beta_{\pm}$ do not depend on the polar angle θ. This yields, in the (e_+,e_-,e_3) basis, the following boundary conditions which can be handled in a classical way (see Appendix A):

$$\begin{aligned}&(\alpha_{\pm}\omega_+ +\beta_{\pm}\,\partial_{\mathrm{n}}\omega_+)|_{\Gamma}=f_+\,,\\ &(\alpha_{\pm}\omega_- +\beta_{\pm}\,\partial_{\mathrm{n}}\omega_-)|_{\Gamma}=f_-\,,\end{aligned} \tag{37}$$

with $f_+=f_1+\mathrm{i}f_2$ and $f_-=f_1-\mathrm{i}f_2$.

Clearly, for boundary conditions different from (35), (36), one has to expect some difficulties. This is the case for the Stokes problem (1), (2), (19). As shown in the following section, we use the influence matrix technique to recover the admissible boundary conditions which have just been defined.

4. Solution of the Stokes problem in cylindrical coordinates

Let us now consider the Stokes problem defined by the vectorial equations (1), (2) associated with the boundary conditions (19). The Poisson equation (2) is a particular case of a Helmholtz equation and so, after Section 3, it is now clear that the difficulties come from the conditions (19). In this section, for each variable ψ and ω, we suggest using an influence matrix technique which permits us to substitute Dirichlet boundary conditions for the conditions which are difficult to handle. The algorithm that we suggest is an extension in 3D of [14, 15] in 2D, where ω and ψ are scalar; it is specially suited in time-dependent situations for which the Stokes problem must be solved at each time step.

4.1. Vector potential equation

For the vector potential one has to impose the scalar and vectorial boundary conditions,

$$\nabla\cdot\psi|_\Gamma = 0\,, \qquad \psi_t|_\Gamma = 0\,, \tag{38}$$

and the difficulty clearly comes from the scalar one which is not simply of Dirichlet type. In cylindrical coordinates and in the physical basis (e_1, e_2, e_3), one has

$$\nabla\cdot\psi = \partial_\rho\psi_1 + \frac{1}{\rho}\psi_1 + \frac{1}{\rho}\partial_\theta\psi_2 + \partial_\zeta\psi_3\,. \tag{39}$$

This yields, in Fourier spectral space,

$$\nabla\cdot\psi(\rho,\zeta;k) = \partial_\rho\hat{\psi}_1 + \frac{1}{\rho}\hat{\psi}_1 + \frac{ik}{\rho}\hat{\psi}_2 + \partial_\zeta\hat{\psi}_3\,. \tag{40}$$

Taking into account for ψ the change of basis defined for ω by Eqs. (21), one obtains in the (e_+, e_-, e_3) basis.

$$\widehat{\nabla\cdot\psi}(\rho,\zeta;k) = \frac{1}{2}\partial_\rho(\hat{\psi}_+ + \hat{\psi}_-) + \frac{1}{2\rho}[(1+k)\hat{\psi}_+ + (1-k)\hat{\psi}_-] + \partial_\zeta\hat{\psi}_3\,. \tag{41}$$

By using the superscripts 1, −1 and 0 for the upper, lower and lateral parts of the $(\rho-\zeta)$ domain, the boundary conditions (38) can be written as

$$\hat{\psi}_+|_{\Gamma^1\cup\Gamma^{-1}} = 0\,, \qquad \hat{\psi}_-|_{\Gamma^1\cup\Gamma^{-1}} = 0\,, \qquad \partial_\zeta\hat{\psi}_3|_{\Gamma^1\cup\Gamma^{-1}} = 0\,, \qquad \hat{\psi}_3|_{\Gamma^0} = 0\,, \tag{42a}$$

$$\widehat{\nabla\cdot\psi}|_{\Gamma^0} = 0\,, \qquad \hat{\psi}_+|_{\Gamma^0} = \hat{\psi}_-|_{\Gamma^0}\,, \tag{42b}$$

with

$$\widehat{\nabla\cdot\psi}|_{\Gamma^0} = \frac{1}{2}\partial_\rho(\hat{\psi}_+ + \hat{\psi}_-) + \frac{1}{R}\hat{\psi}_+|_{\Gamma^0} \quad (R \text{ is the cylinder radius})\,.$$

In the approach described in Section 3 for solving the Helmholtz vectorial equation, the boundary conditions have been considered as expressed by Eqs. (35), (36). This hypothesis is fully satisfied for the $\hat{\psi}_3$ component, with the homogeneous Dirichlet and Neumann boundary conditions (42a). Concerning the $\hat{\psi}_+$ and $\hat{\psi}_-$ components, conditions (42a) are admissible but not (42b). Clearly, if no coupling occurs between the equations for $\hat{\psi}_+$ and $\hat{\psi}_-$, the coupling now occurs through the boundary conditions. To overcome this difficulty and thus avoid the simultaneous resolution of the two equations, we use an algorithm specially attractive when multiple resolutions are needed.

In Fourier spectral space and with $\hat{\omega}$ given, let us consider for the + and − components, the solutions $\hat{\psi}^{(1)}$ and $\hat{\psi}^{(2)}$ of the problems P_1 and P_2 such that

problem P_1:

$$\Delta_k^+ \hat{\psi}_+^{(1)} + \hat{\omega}_+ = 0\,, \qquad \Delta_k^- \hat{\psi}_-^{(1)} + \hat{\omega}_- = 0\,,$$
$$\hat{\psi}_+^{(1)}|_\Gamma = 0\,, \qquad \hat{\psi}_-^{(1)}|_\Gamma = 0\,; \tag{43}$$

problem P_2:

$$\Delta_k^+ \hat{\psi}_+^{(2)} = 0\,, \qquad \Delta_k^- \hat{\psi}_-^{(2)} = 0\,,$$
$$\hat{\psi}_+^{(2)}|_{\Gamma^1 \cup \Gamma^{-1}} = 0\,, \qquad \hat{\psi}_-^{(2)}|_{\Gamma^1 \cup \Gamma^{-1}} = 0\,,$$
$$\hat{\psi}_+^{(2)}|_{\Gamma^0} = \hat{\psi}_-^{(2)}|_{\Gamma^0} \text{ such that } \widehat{\nabla \cdot \psi}^{(1)} + \widehat{\nabla \cdot \psi}^{(2)}|_{\Gamma^0} = 0\,, \tag{44}$$

in such a way that $\hat{\psi}_+ = \hat{\psi}_+^{(1)} + \hat{\psi}_+^{(2)}$, $\hat{\psi}_- = \hat{\psi}_-^{(1)} + \hat{\psi}_-^{(2)}$ are solution of the complete problem.

In transient situations, the advantage of splitting the complete problem into problems P_1 and P_2 is that the time dependent vorticity is considered in problem P_1, which can easily be solved. The boundary conditions of the problem P_2 can now be computed by using the influence matrix technique.

The basic idea is to compute once a set of elementary solutions which will be linearly combined, as often as needed, in order to constitute the solution of problem P_2. More precisely, after discretization of the $(\rho-\zeta)$ plane (see Appendix A), the values along Γ^0 of a function as $\hat{\psi}_+^{(2)}$, which is for continuity reasons equal to zero in the corners, i.e. at $\Gamma^0 \cap \Gamma^1$ and $\Gamma^0 \cap \Gamma^{-1}$, is entirely defined by $(I-1)$ values for the real or imaginary part of each mode number k (the collocation point number in ζ is equal to $I+1$). If one considers the corresponding vector space of dimension $I-1$, there exists a linear operator $\mathbb{F}_k$ associated with problem P_2 and the definition of the divergence in the (e_+, e_-, e_3) basis such that

$$\mathrm{Re}\{\widehat{\nabla \cdot \psi}^{(2)}|_{\Gamma^0}\} = \mathbb{F}_k[\mathrm{Re}\{\hat{\psi}_+^{(2)}|_{\Gamma^0}\}]\,, \qquad \mathrm{Im}\{\widehat{\nabla \cdot \psi}^{(2)}|_{\Gamma^0}\} = \mathbb{F}_k[\mathrm{Im}\{\hat{\psi}_+^{(2)}|_{\Gamma^0}\}]\,. \tag{45}$$

The existence of this operator results from: (i) the linearity of the Poisson vectorial equation; (ii) the real character of the vectorial Laplacian and divergence operators in the (e_+, e_-, e_3) basis; and (iii) the equality $\hat{\psi}_-^{(2)}|_{\Gamma^0} = \hat{\psi}_+^{(2)}|_{\Gamma^0}$. Such an operator can be easily produced by computing the canonical basis of the vector space under consideration.

Assuming that the operator $\mathbb{F}_k$ is regular (numerically confirmed) the inverse operator $\mathbb{F}_k^{-1}$ exists. Using the results of problem P_1, it enables the computation of the boundary conditions of problem P_2, as well as those of the complete problem,

$$\mathrm{Re}\{\hat{\psi}_+|_{\Gamma^0}\} = \mathbb{F}_k^{-1}[\mathrm{Re}\{-\widehat{\nabla \cdot \psi}^{(1)}|_{\Gamma^0}\}]\,, \qquad \mathrm{Im}\{\hat{\psi}_+|_{\Gamma^0}\} = \mathbb{F}_k^{-1}[\mathrm{Im}\{-\widehat{\nabla \cdot \psi}^{(1)}|_{\Gamma^0}\}]\,. \tag{46}$$

The discretized form of the $\mathbb{F}_k$ operator is the influence matrix, of dimension $I-1 \times I-1$.

4.2. Vorticity equation

The boundary conditions that must be considered for determining the vorticity are

$$\nabla \cdot \omega|_\Gamma = 0\,, \qquad v_t|_\Gamma = 0\,. \tag{47}$$

Let us recall first the expression of the velocity, as the curl of the vector potential, in the basis (e_1, e_2, e_3):

$$v = \left(\frac{1}{\rho}\partial_\theta \psi_3 - \partial_\zeta \psi_2\right) e_1 + (\partial_\zeta \psi_1 - \partial_\rho \psi_3) e_2 + \left(\partial_\rho \psi_2 + \frac{1}{\rho}\psi_2 - \frac{1}{\rho}\partial_\theta \psi_1\right) e_3\,. \tag{48}$$

This yields, in Fourier spectral space,

$$\hat{v}(\rho, \zeta; k) = \left(\frac{\mathrm{i}k}{\rho}\hat{\psi}_3 - \partial_\zeta \hat{\psi}_2\right) e_1 + (\partial_\zeta \hat{\psi}_1 - \partial_\rho \hat{\psi}_3) e_2 + \left(\partial_\rho \hat{\psi}_2 + \frac{1}{\rho}\hat{\psi}_2 - \mathrm{i}\frac{k}{\rho}\hat{\psi}_1\right) e_3 \tag{49}$$

and in the (e_+, e_-, e_3) basis,

$$\hat{v} = \mathrm{i}\Big[\Big(\frac{k}{\rho}\hat{\psi}_3 + \partial_\zeta\hat{\psi}_+ - \partial_\rho\hat{\psi}_3\Big)e_+ + \Big(\partial_\rho\hat{\psi}_3 + \frac{k}{\rho}\hat{\psi}_3 - \partial_\zeta\hat{\psi}_-\Big)e_- - \frac{1}{2}\Big(\partial_\rho(\hat{\psi}_+ - \hat{\psi}_-) + \frac{1}{\rho}((k+1)\hat{\psi}_+ + (k-1)\hat{\psi}_-)\Big)e_3\Big]. \tag{50}$$

Knowing that along the boundary Γ the normal component of the velocity vanishes, the boundary condition (47) for its tangential component can be written as

$$\hat{v}_+|_\Gamma = 0\,, \qquad \hat{v}_-|_{\Gamma^1\cup\Gamma^{-1}} = 0\,, \qquad \hat{v}_3|_{\Gamma^0} = 0\,, \tag{51}$$

where again we split Γ into Γ^{-1}, Γ^1 and Γ^0.

Such boundary conditions are clearly not admissible since they do not involve the vorticity directly but the derivatives of the vector potential; so, we again suggest the use of an influence matrix technique, in order to obtain Dirichlet boundary conditions on the vorticity. Moreover, it has been shown in the previous section that it is not easy to ensure the homogeneous divergence condition on the circular part of the cylinder. In the approach that we describe now the influence matrix technique permits us to handle all the non-admissible boundary conditions.

Once again, using the linearity property of the complete problem, we split it into two problems P_1 and P_2 such as:

problem P_1:

$$\begin{aligned}
&\Delta_k^+\hat{\omega}_+^{(1)} - \sigma\hat{\omega}_+^{(1)} = \hat{w}_+\,,\\
&\Delta_k^-\hat{\omega}_-^{(1)} - \sigma\hat{\omega}_-^{(1)} = \hat{w}_-\,,\\
&\Delta_k\hat{\omega}_3^{(1)} - \sigma\hat{\omega}_3^{(1)} = \hat{w}_3\,,\\
&\hat{\omega}_+^{(1)}|_\Gamma = 0\,, \qquad \hat{\omega}_-^{(1)}|_\Gamma = 0\,; \qquad \widehat{\nabla\cdot\omega}^{(1)}|_{\Gamma^1\cup\Gamma^{-1}} = \partial_\zeta\hat{\omega}_3^{(1)}|_{\Gamma^1\cup\Gamma^{-1}} = 0\,; \qquad \hat{\omega}_3^{(1)}|_{\Gamma^0} = 0\,;
\end{aligned} \tag{52}$$

problem P_2:

$$\begin{aligned}
&\Delta_k^+\hat{\omega}_+^{(2)} - \sigma\hat{\omega}_+^{(2)} = 0\,,\\
&\Delta_k^-\hat{\omega}_-^{(2)} - \sigma\hat{\omega}_-^{(2)} = 0\,,\\
&\Delta_k\hat{\omega}_3^{(2)} - \sigma\hat{\omega}_3^{(2)} = 0\,,\\
&\widehat{\nabla\cdot v}^{(2)}|_{\Gamma^1\cup\Gamma^{-1}} = 0\,; \qquad \hat{\omega}_+^{(2)}|_\Gamma,\ \hat{\omega}_-^{(2)}|_\Gamma,\ \hat{\omega}_3^{(2)}|_{\Gamma^0} \text{ such that}\\
&\hat{v}_+^{(2)} + \hat{v}_+^{(1)}|_\Gamma = 0\,; \qquad \hat{v}_-^{(2)} + \hat{v}_-^{(1)}|_{\Gamma^1\cup\Gamma^{-1}} = 0\,; \qquad \hat{v}_3^{(2)} + \hat{v}_3^{(1)}|_{\Gamma^0} = 0\,; \qquad \widehat{\nabla\cdot\omega}^{(2)} + \widehat{\nabla\cdot\omega}^{(1)}|_{\Gamma^0} = 0\,.
\end{aligned} \tag{53}$$

As previously for the vector potential the resolution of the problem P_1 can be achieved easily and for the problem P_2 the influence matrix technique is employed.

After the discretization in space, taking into account that the no slip boundary condition induces $\hat{\omega}_+$, $\hat{\omega}_-$ and $\hat{\omega}_3$ to be equal to zero in the corners, for the real or imaginary part of each Fourier mode k the number of unknown values of $\hat{\omega}$ along Γ is $4J' + 3(I-1)$ ($J'+1$ is the collocation point number until the axis, see Appendix A). Considering the vector space of same dimension, for each mode number k one can exhibit a linear operator $\mathbb{H}_k$, such that

$$[\mathrm{Im}\{\hat{v}_+^{(2)}|_\Gamma, \hat{v}_-^{(2)}|_{\Gamma^1\cup\Gamma^{-1}}, \hat{v}_3^{(2)}|_{\Gamma^0}\}, \mathrm{Re}\{\widehat{\nabla\cdot\omega}^{(2)}|_{\Gamma^0}\}] = \mathbb{H}_k[\mathrm{Re}\{\hat{\omega}_+^{(2)}|_\Gamma, \hat{\omega}_-^{(2)}|_\Gamma, \hat{\omega}_3^{(2)}|_{\Gamma^0}\}] \tag{54a}$$

$$[\mathrm{Re}\{-\hat{v}_+^{(2)}|_\Gamma, -\hat{v}_-^{(2)}|_{\Gamma^1\cup\Gamma^{-1}}, -\hat{v}_3^{(2)}|_{\Gamma^0}\}, \mathrm{Im}\{\widehat{\nabla\cdot\omega}^{(2)}|_{\Gamma^0}\}] = \mathbb{H}_k[\mathrm{Im}\{\hat{\omega}_+^{(2)}|_\Gamma, \hat{\omega}_-^{(2)}|_\Gamma, \hat{\omega}_3^{(2)}|_{\Gamma^0}\}] \tag{54b}$$

The existence of this operator results from: (i) the linearity of the Helmholtz and Poisson vectorial equations; (ii) the linearity of the curl and divergence operators; and (iii) in the (e_+, e_-, e_3) basis, from the imaginary character of the curl operator and the real character of the other operators. One can

notice in (54b) the sign inversion of the velocity components, due to the imaginary character of the curl operator.

As previously, the most efficient way to define the operator $\mathbb{H}_k$ is to compute the image of the canonical basis of the vector space which has been introduced.

In order to determine the boundary conditions on $\hat{\omega}$ for problem P_2 starting from the results of problem P_1, one has to invert the $\mathbb{H}_k$ operators. The difficulty comes here from the mode number $k=0$ for which $\mathbb{H}_k$ is not regular, with a kernel of dimension 2.

The non-regular character of $\mathbb{H}_k$ for $k=0$ can be understood by analyzing the implications in the corners of the velocity field properties. For problem P_2, as well as for all the elementary solutions of the influence matrix, the expression of the velocity as the curl of a vector field perpendicular to the boundary induces in the corners $C^1(\Gamma^1 \cap \Gamma^0)$ and $C^{-1}(\Gamma^{-1} \cap \Gamma^0)$ is

$$\hat{v}_1^{(2)}|_{C^\mu} = \hat{v}_3^{(2)}|_{C^\mu} = 0\,, \quad \mu = -1, 1 \tag{55}$$

and, as a result of the solenoidal character of the velocity field, the so-called 'compatibility equations' are

$$\partial_\rho \hat{v}_1^{(2)} + \frac{1}{\rho}\,\hat{v}_1^{(2)} + \partial_\zeta \hat{v}_3^{(2)} + \mathrm{i}k\hat{v}_2^{(2)}|_{C^\mu} = 0\,, \quad \mu = -1, 1\,. \tag{56}$$

For $k=0$, these 'compatibility equations' imply that $\hat{v}_1^{(2)}$ along Γ^1 and Γ^{-1}, and $\hat{v}_3^{(2)}$ along Γ^0 are dependent. In the discretized framework, their spectral approximations produce two linear relations between the collocation point values; for example if the collocation point values of $\hat{v}_3^{(2)}$ along Γ^0 are given, then a linear relations occurs between the collocation point values of $\hat{v}_1^{(2)}$ along Γ^1 and a similar one for $\hat{v}_1^{(2)}$ along Γ^{-1}. The kernel of the operator $\mathbb{H}_{k=0}$ is then at least of dimension 2.

One way to proceed with the singular character of the operator $\mathbb{H}_{k=0}$ is to produce a regular operator $\mathbb{H}'_{k=0}$ close to $\mathbb{H}_{k=0}$. Considering the matrix associated with $\mathbb{H}_{k=0}$ and the equations associated with each line of this matrix, such a goal can be achieved by the suppression of two equations and their replacement. The previous analysis suggests suppressing one equation relative to the value of $\hat{v}_1^{(2)}$ at a collocation point of Γ^1 and another one for the value of $\hat{v}_1^{(2)}$ at a collocation point of Γ^{-1}. Thus, in the (e_+, e_-, e_3) basis, we have suppressed the equations relative to $\hat{v}_+^{(2)}$ along Γ^1 and Γ^{-1} at the collocation points nearest to the corners C^1 and C^{-1}. In order to recover a square matrix one has to produce two new equations; using Lagrange interpolation polynomials we force the spectral approximations of $\hat{\omega}_+$ along Γ^1 and Γ^{-1} to be of the lowest degree.

One can now control that $\mathbb{H}'_{k=0}$ is really close to $\mathbb{H}_{k=0}$ in the sense that the no slip boundary condition is well imposed at all the collocation points, including the collocation points of Γ^1 and Γ^{-1}, the nearest to the corners. In Fourier spectral space, for the mode number $k=0$, the real character of the velocity field induces

$$\mathrm{Re}(\hat{v}_+) = \mathrm{Re}(\hat{v}_-) = \hat{v}_1\,, \qquad \mathrm{Im}(\hat{v}_+) = -\mathrm{Im}(\hat{v}_-) = \hat{v}_2\,. \tag{57}$$

Then, using the influence matrix technique, when one imposes at all the collocation points of Γ^1 and Γ^{-1},

$$\hat{v}_-^{(1)} + \hat{v}_-^{(2)} = 0\,, \tag{58}$$

one also imposes along Γ^1 and Γ^{-1} the set of equations,

$$\hat{v}_+^{(1)} + \hat{v}_+^{(2)} = 0\,, \tag{59}$$

which includes the two equations which have been taken out. Thus, as expected, the tangential components of the velocity are well null at all the collocation points of Γ^1 and Γ^{-1}.

5. Vorticity correction algorithm and numerical test

The first numerical tests of the Stokes solver developed on the bases of the previous sections have been disappointing; if the solutions, ω and ψ, of the Stokes problem are not 2D axisymmetric or 3D analytic polynomial, then some drawbacks occur that we can summarize as follows:

- the basic equation (13) is not exactly verified, specially in the vicinity of the corners C^1 and C^{-1}; in our vorticity–vector potential approach, this results in the coherency problem where the computed vorticity is not exactly the curl of the computed velocity;
- ω and ψ are not solenoidal; $\nabla\cdot\omega$ and $\nabla\cdot\psi$ show oscillating values with amplitudes increasing in the vicinity of the corners;
- the boundary values of the normal component of ω show weak oscillations, specially near the corners, instead of being equal to zero;
- the boundary values of the tangential component of ω are very unregular near the corners, specially along Γ^1 and Γ^{-1}; a spectral analysis of the influence matrices has shown us that this point is not problem dependent; the influence matrices $\mathbb{H}_k$ are ill conditioned and exhibit small eigenvalues associated with eigenvectors which geometrically relate to the collocation points near the corners.

These drawbacks can be attributed to (i) a regularity failure of the vorticity at the corners or (ii) to the loss of some basic properties of the continuous equations through their spectral approximation. Concerning point (i), it is known [16] that in a two-dimensional $\pi/2$ angle, the vorticity exhibits an infinity of oscillations; in Section 5.1., we focus on point (ii) and suggest a 'vorticity correction algorithm' in order to produce more satisfying solutions. In Section 5.2. our Stokes solver is tested in a 3D Rayleigh-Bénard convective problem.

5.1. *Vorticity correction algorithm*

As shown in Section 2, the basic equation (13) results from the Stokes problem (1), (2), (19) due to Eqs. (14) and (15) and to the identity (5). In the discretized framework, such equations are no longer valid, due to (i) the cylindrical coordinate system and to (ii) the collocation spectral method itself.

Due to the ρ^{-1} term in the curl and vectorial laplacian operators, the discretized form of the identity (5) becomes approximate; for the same reason, the commutativity property of the divergence and Laplacian operator, used to obtain Eqs. (14) and (15), is no longer absolutely right. Without going into the details, but in order to clearly mention these difficulties, one may observe that the identity

$$\frac{1}{\rho}\,\partial_\rho \rho\omega_1 = \partial_\rho \omega_1 + \frac{\omega_1}{\rho} \tag{60}$$

is not exact when using the spectral formulation of the ∂_ρ operator (see Appendix A), except where ω_1 is a polynomial with degree small enough considering the number of collocation points. Such an approximation is even less accurate when using coordinate transforms or the change of variable introduced in Section 3.

Eqs. (14) and (15) are also altered by another error due to the fact that the discretized equations are not expressed on the boundary, when using the collocation method (see Appendix A). Such an error can be clearly pointed out by introducing a τ vector term, null everywhere except at the collocation points of the boundary, and writing, e.g. for the vorticity equation:

$$\nabla^2\omega - \sigma\omega = w + \tau\,, \tag{61}$$

with ∇^2 the discretized form of the Laplacian operator. By using now the discretized divergence operator and neglecting the approximation due to the cylindrical coordinate system, one obtains

$$\nabla^2(\nabla\cdot\omega) - \sigma(\nabla\cdot\omega) = \nabla\cdot\tau\,. \tag{62}$$

The solution $\nabla\cdot\omega$ of this non-homogeneous Helmholtz equation, associated with homogeneous boundary conditions, is not null; the solenoidal character of ω is thus no longer imposed.

When using the velocity pressure formulation, solutions have been introduced, first in 1D [17] and later in 2 and 3D [12]. The basic ideas are (i) to start from the discretized form of the momemtum equation, (ii) to constitute for the pressure an equation in which the τ term is involved and (ii) to use an extended influence matrix technique in order to anticipate the τ values. Unfortunately, such an approach is not possible in the vorticity–vector potential formulation for which all the vector fields are implicitly solenoidal, in contrast to the velocity–pressure formulation for which a degree of freedom, the pressure, is associated with the continuity equation. Nevertheless, in order to make the tau error

smaller, an approach similar to the one introduced in [18] is possible; it consists of imposing at the boundary not only the boundary condition but a linear combination of this condition and of the partial derivative equation itself; although promising in different contexts the first results we have obtained seem disappointing.

The vorticity correction we suggest to overcome these difficulties is specially interesting for time dependent problems, in order to avoid possible error cumulations; it consists of substituting for ω, from the resolution of the Stokes problem, a vectorial field ω' equal to the vorticity definition (3). Neglecting again the approximations due to the cylindrical coordinate system, one can write

$$\omega' - \omega = \nabla \times \nabla \times \psi + \nabla^2 \psi = \nabla(\nabla \cdot \psi) . \tag{63}$$

The drawback is that the vorticity equation is no longer exactly verified, but such an approximation is not so unusual. For example, with the velocity–pressure formulation, the momentum equation cannot be longer perfectly verified when using a basis of divergence free functions for the velocity, in order to impose the continuity equation [19]. Another example, very close to our problem, can be found when considering the Maxwell equations for which the electric and magnetic fields are implicitly divergence free; in [20, 21] Lagrange multipliers, looking like electric and magnetic correcting potentials or some pressures in fluid mechanics, are introduced in the governing equations in order to consider explicitly the divergence free constraints. This last approach must be rejected in our case, since the vorticity–vector potential formulation is essentially chosen in order to avoid the treatment of the pressure and continuity equation.

5.2. *Numerical test*

Beyond the elementary tests of the informatical implementation of our Stokes solver, it was interesting to control the quality of our results in the framework of a physical problem. To this end, we come back to a numerical experiment of Rayleigh–Bénard convection in a vertical cylinder [22], using the Boussinesq approximation. Let us recall [22] that the Stokes problem which has to be solved at each time-step results from the use of an implicit three level approximation of the time derivative, a full implicit evaluation of the diffusive term and an explicit Adams–Bashforth extrapolation for the non-linear convective term, i.e. $\nabla \times (\omega \times v)$ by using the conservative form. The force term w of the vorticity equation also involves in an implicit manner the buoyancy term Ra $(\nabla \times Te_3)$, where Ra is the Rayleigh number and T the temperature. For the temperature equation, solved at each time-step

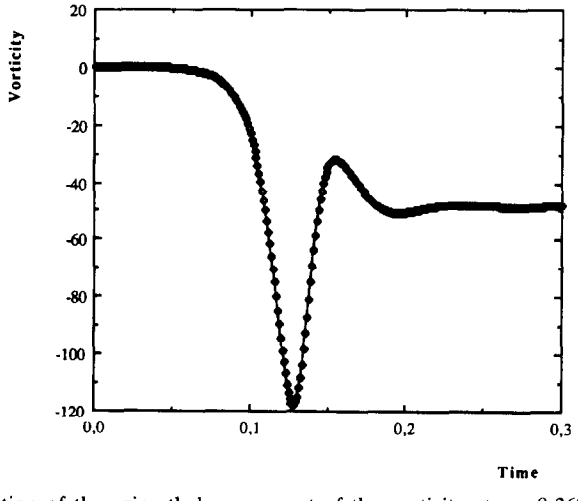

Fig. 1. Evolution of the azimuthal component of the vorticity at $\rho = 0.362$, $\theta = 0$, $\zeta = 0$.

before solving the Stokes problem, the same approximations are used, both for the linear terms and for the non-linear term $v \cdot \nabla T$.

Let us now describe the numerical experiment:

- Boundary conditions: for temperature, Dirichlet conditions at the bottom and at the top of the cylinder (1 and 0 in dimensionless form), homogeneous Neumann conditions on the lateral wall; for velocity, no slip condition everywhere;
- Initial condition: conductive state, i.e. linear variation of the temperature along ζ;
- Fluid: Prandtl number Pr = 6.7 (water);
- Aspect ratio (ratio of the cylinder diameter to its height) Ar = 1.

As usual in natural convection, the Rayleigh number Ra is the leading parameter of the convective flow. With Ar = 1, as predicted by the linear stability theory, the critical Ra is about 3800 and beyond the only stationary solution is 3D and constituted with one roll around a horizontal axis (e.g. $\theta = \pi/2$,

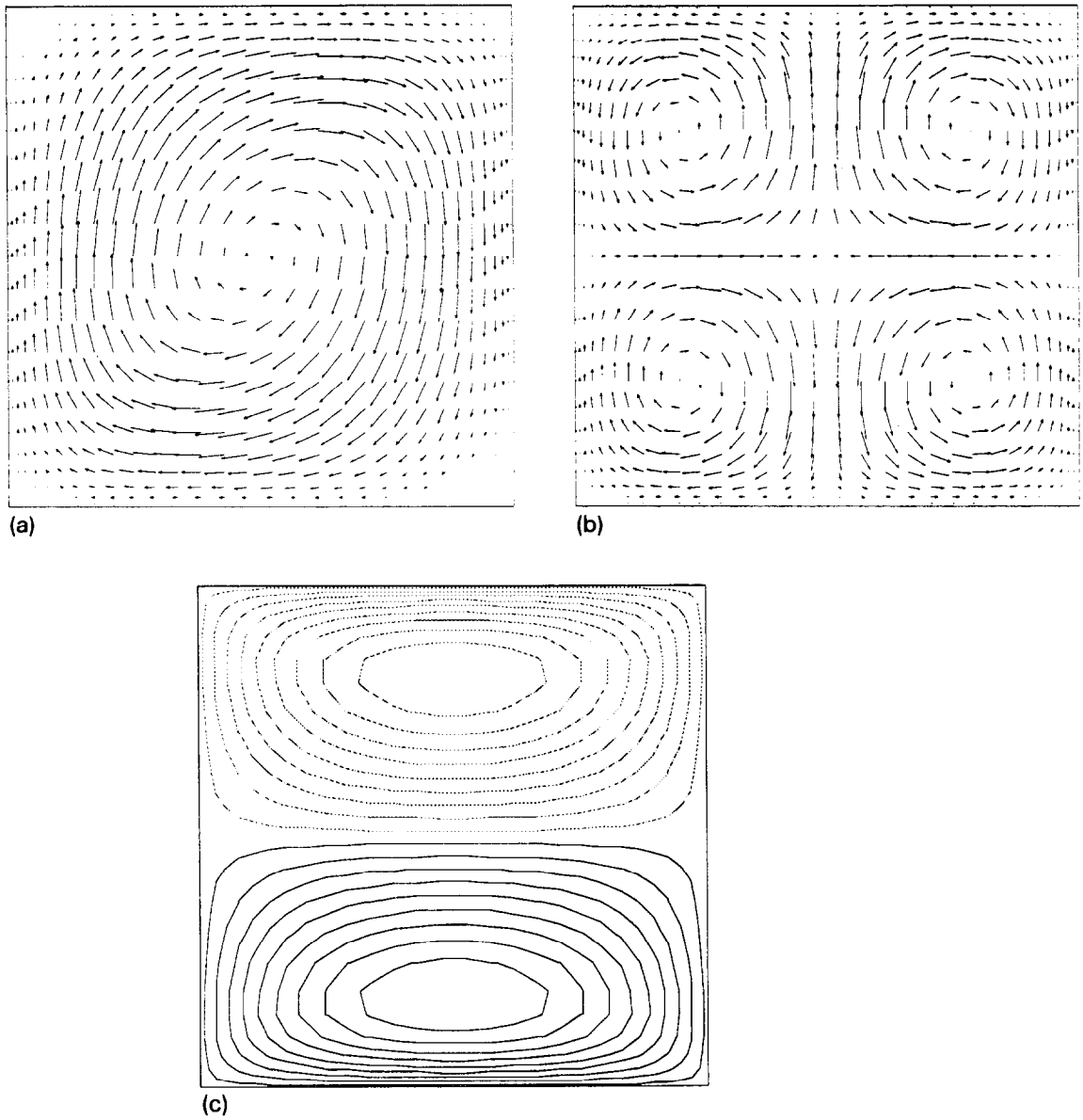

Fig. 2. (a) Velocity in the P1 plane; maximum value = 36.168. (b) Tangential component of the velocity in the P2 plane; maximum value = 9.032. (c) Normal component of the velocity in the P2 plane; $-28.676 \leq v_2 \leq 28.676$.

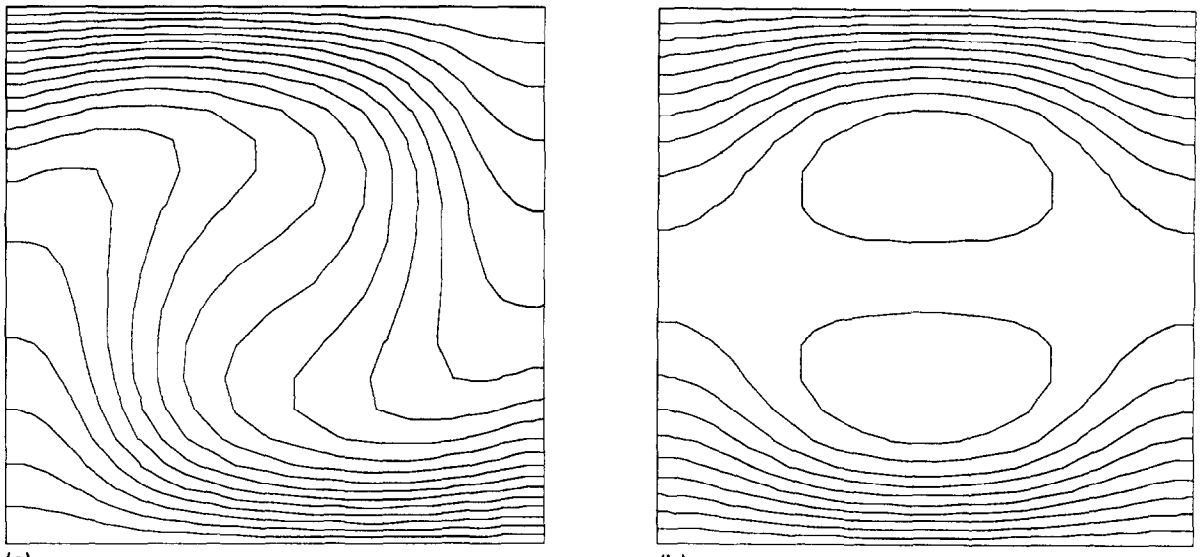

Fig. 3. (a) Temperature in the P1 plane: $0 \leq T \leq 1$. (b) Temperature in the P2 plane: $0 \leq T \leq 1$.

$\zeta = 0$) and corresponds essentially to the mode $k = 1$. As in [23], we have computed the 3D stationary solution obtained with Ra = 17500 (see also [24] for similar calculations). The following time and space discretizations have been used:

- time step (dimensionless form using the thermal diffusivity): 10^{-3}
- collocation point number: 17 in ρ ($0 \leq \rho \leq 0.5$, $J = 16$), 25 in $\zeta(-0.5 \leq \zeta \leq 0.5$, $I = 24$) and 16 in θ.

In Fig. 1 is presented the evolution of the vorticity (azimuthal component ω_2) in the plane of symmetry $\theta = 0$, π at the particular point where $\rho = 0.362$, $\zeta = 0$. The results are presented in Figs. 2–5 for the 3D stationary state, obtained approximately at $t = 0.3$. For each of the unknowns, we give visualizations in the two perpendicular planes P1: $\theta = 0$, π and P2: $\theta = \pi/2$, $3\pi/2$.

In Fig. 2(a) is shown the velocity in the symmetry plane P1, for which the normal component v_2 is null. In the perpendicular plane P2, the tangential component is given in Fig. 2(b) and the normal component in Fig. 2(c). As expected, the flow is essentially constituted with a roll around a horizontal axis, but one can observe, as in [23], the superimposition in the plane P2 of a secondary flow consisting of four symmetric rolls.

In Fig. 3(a) and (b) is shown the temperature in the planes P1 and P2. The primary flow induces a distortion of the isotherms clearly pointed out in Fig. 3(a); in Fig. 3(b) one observes that this distortion decreases with the distance to the circular wall of the cylinder.

The results obtained for the vorticity are presented in Fig. 4. In Fig. 4(a) is shown the ω_2 component in the symmetry plane P1, for which the tangential component is null; the results obtained in the plane P2 are given in Fig. 4(b), for the tangential component of the vorticity, and 4(c), for its normal component. One can notice in Fig. 4(b) that, as expected, the vorticity field is tangential to the walls.

Similar results are presented in Fig. 5 for the vector potential. In Fig. 5(a) is shown the ψ_2 component in the plane P1, for which ψ_1 and ψ_3 are null, and the results obtained in the plane P2 are given in Fig. 5(b), for the tangential component, and Fig. 5(c), for the normal component. In contrast to the vorticity field, the vector potential field is clearly normal to the walls, as shown in Fig. 5(b).

The present results have been obtained using the vorticity correction algorithm. As already mentioned, this correction induces that the vorticity equation is not accurately verified. In order to test if the correction algorithm does not have a drastic effect on the results, we have compared the solutions obtained with and without this correction. Quantitative results are proposed in Table 1, corresponding to time $t = 0.3$. In this table are given for the two solutions and for their deviation, the mean quadratic value, the maximum and minimum values of the different scalar and vector fields (for which the

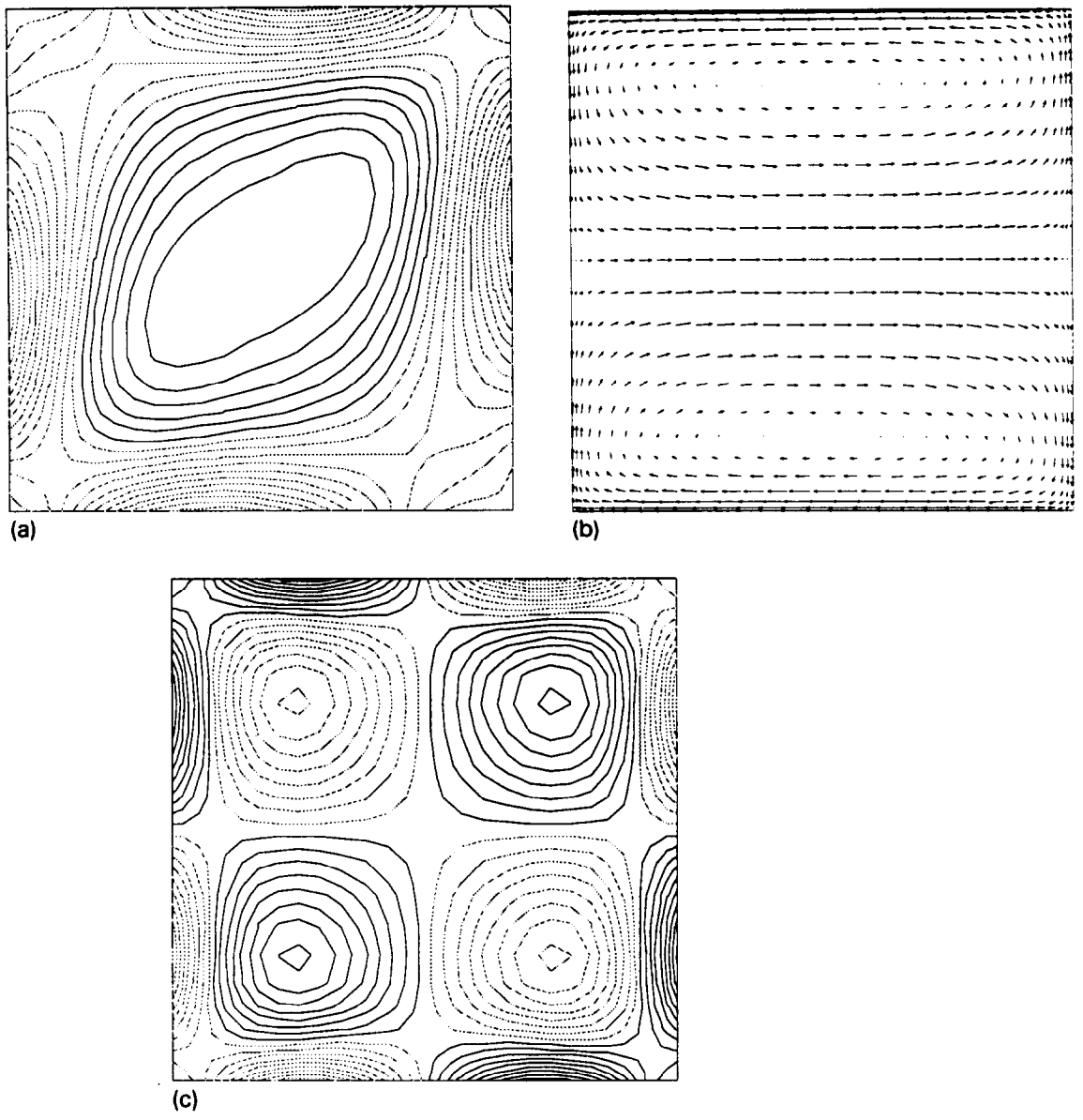

Fig. 4. (a) Vorticity in the P1 plane; $-456.22 \leq \omega_2 \leq 257.60$. (b) Tangential component of the vorticity in the P2 plane; maximum value = 386.34. (c) Normal component of the vorticity in the P2 plane; $-118.05 \leq \omega_2 \leq 118.05$.

modulus are considered) and their localization inside the cylinder ($1 \leq z$ index $\leq I - 1 = 23$, $1 \leq r$ index $\leq J' = 16$, $0 \leq \theta$ index $\leq 2K - 1 = 31$, see Eqs. (A.3) in Appendix A). Such results appear satisfying:

– the relative deviations are less than 10^{-3} for the velocity and temperature;

– the localizations of all the significative maxima and minima are not altered.

6. Conclusion

A spectral algorithm to solve the Stokes problem in vorticity–vector potential formulation and cylindrical geometry has been proposed. For all the non-trivial tasks:

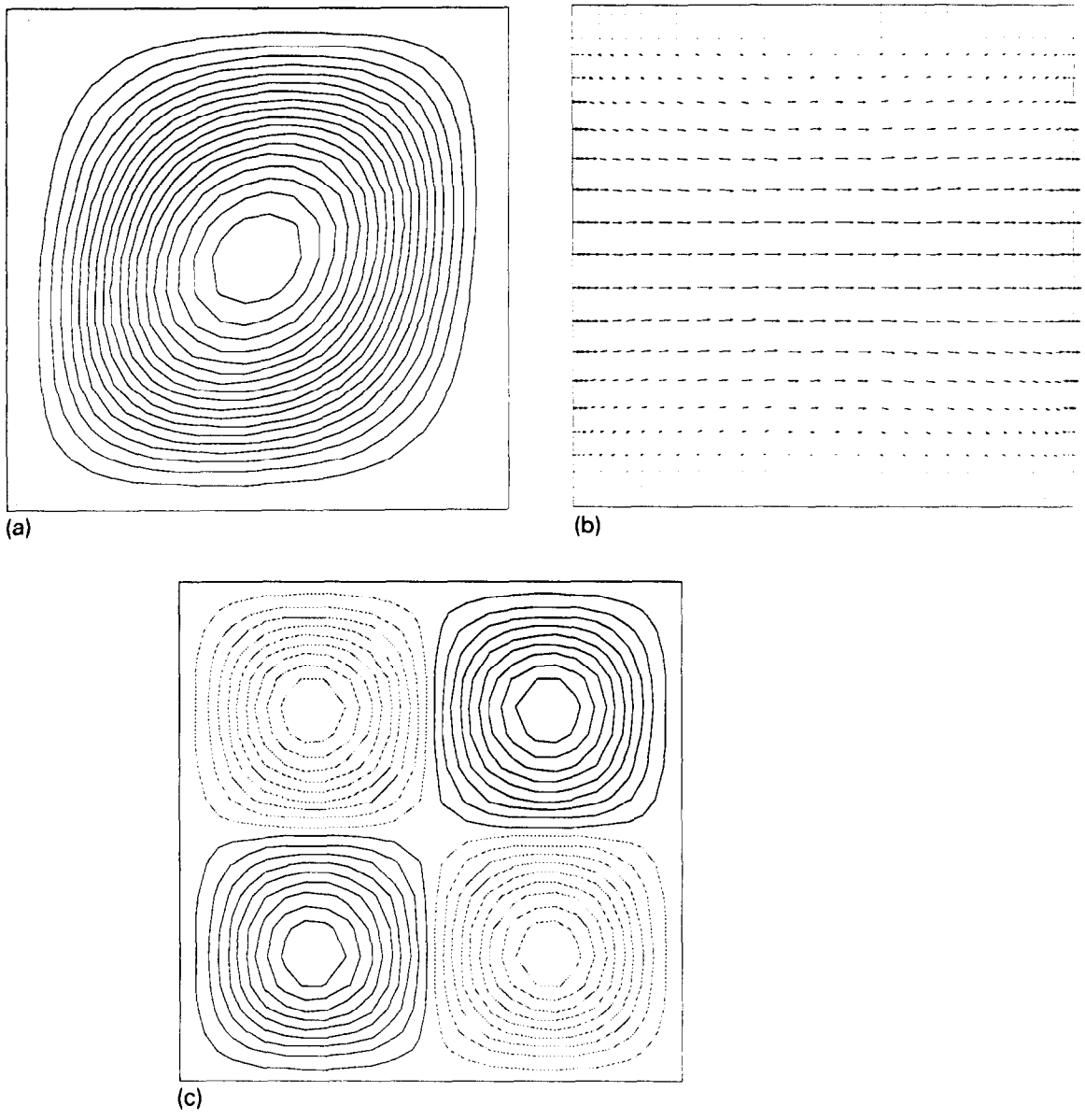

Fig. 5. (a) Vector potential in the P1 plane; $-0.082 \leq \psi_2 \leq 8.021$. (b) Tangential component of the vector potential in the P2 plane; maximum value–8.040. Normal component of the vector potential in the P2 plane; $-0.816 \leq \psi_2 \leq 0.816$.

- inherent to the cylindrical coordinate system,
- involved by the use of influence matrices for the boundary conditions,
- due to the solenoidal character of all the vectorial fields, our procedures have been described with going into the details.

A numerical test of this Stokes solver has been proposed, in the framework of a 3D Rayleigh–Bénard convection problem. In particular, it has been pointed out that the discretized forms of the equations induce specific problems that the use of a vorticity correction algorithm permits us to overcome in a satisfactory way.

Let us also mention that the numerical method has already been employed for less academic problems, specially for simulations of thermal plumes and double diffusive convection, for which fine meshes and coordinate transforms are required [25, 26].

Table 1
Comparison of the results obtained with and without the vorticity correction algorithm

With correction ($t = 0.3$)	Without correction ($t = 0.3$)	Deviation ($t = 0.3$)
OMEGA	OMEGA	DEV OMEGA
MEAN: 0.17347E + 03	MEAN: 0.17347E + 03	MEAN: 0.29732E + 00
MAX: 0.44862E + 03 (11, 1, 0)	MAX: 0.44862E + 03 (11, 1, 0)	MAX: 0.24029E + 01 (1, 1, 12)
MIN: 0.11565E + 00 (1, 1, 8)	MIN: 0.74459E − 01 (1, 1, 8)	MIN: 0.50043E − 04 (16, 1, 8)
PSI	PSI	DEV PSI
MEAN: 0.29028E + 01	MEAN: 0.29028E + 01	MEAN: 0.14153E − 03
MAX: 0.80398E + 01 (12, 16, 4)	MAX: 0.80396E + 01 (12, 16, 4)	MAX: 0.26631E − 03 (1, 10, 12)
MIN: 0.10925E − 03 (23, 1, 8)	MIN: 0.10930E − 0.3 (23, 1, 8)	MIN: 0.46641E-07 (23, 1, 8)
VELOCITY	VELOCITY	DEV VELOCITY
MEAN: 0.15265E + 02	MEAN: 0.15265E + 02	MEAN: 0.12604E − 03
MAX: 0.36168E + 02 (12, 9, 0)	MAX: 0.36169E + 02 (12, 9, 0)	MAX: 0.28361E − 03 (13, 12, 4)
MIN: 0.57284E − 03 (1, 1, 8)	MIN: 0.57944E − 03 (1, 1, 8)	MIN: 0.73227E − 08 (12, 1, 4)
TEMPERATURE	TEMPERATURE	DEV TEMPERATURE
MEAN: 0.57841E + 00	MEAN: 0.57841E + 00	MEAN: 0.63961E − 06
MAX: 0.99674E + 00 (23, 1, 8)	MAX: 0.99674E + 00 (23, 1, 8)	MAX: 0.18108E − 05 (15, 5, 5)
MIN: 0.32598E − 02 (1, 1, 0)	MIN: 0.32598E − 02 (1, 1, 0)	MIN: −0.18233E − 05 (9, 5, 3)

Acknowledgment

This work was supported by DRET contract 90/218. The calculations have been performed on the CRAY2 computer of CCVR and CRAY-YMP computer of the IMT.

Appendix A

Here the Chebyschev–Chebyschev collocation method that we use for solving the Helmholtz equation (34) in cylindrical geometry is described.

First, let us recall that Chebyshev collocation points are not arbitrary: $(\cos j\pi/J, \cos i\pi/I)$, $0 \leqslant i \leqslant I$, $0 \leqslant j \leqslant J$ for the Gauss–Lobatto points in the (ρ, ζ) plane. If such a mapping is not suitable, it is necessary to use a scaling, or more generally coordinates transforms. With (r, z) defined on $[-1, 1]^2$, assuming that $r(\rho)$ and $z(\zeta)$ are two functions twice derivable and that $r(\rho)$ is even in ρ, one can express the operators $\partial_{\rho\rho}$, ∂_ρ and $\partial_{\zeta\zeta}$ with respect to ∂_{rr}, ∂_r, ∂_z and ∂_{zz}; Then, Eq. (34) yields

$$(\Delta'_{k,m} - \sigma)\tilde{\omega}_3(r, z; k) = \tilde{w}_3(r, z; k)\,, \quad 0 \leqslant k \leqslant K\,, \tag{A.1}$$

with

$$\Delta'_{k,m} = \left(\frac{\mathrm{d}r}{\mathrm{d}\rho}\right)^2 \partial_{rr} + \left(\frac{\mathrm{d}^2 r}{\mathrm{d}\rho^2} + \frac{(2m+1)}{\rho}\frac{\mathrm{d}r}{\mathrm{d}\rho}\right)\partial_r + \left(\frac{\mathrm{d}z}{\mathrm{d}\zeta}\right)^2 \partial_{zz} + \frac{\mathrm{d}^2 z}{\mathrm{d}\zeta^2}\partial_z - \frac{k^2 - m^2}{\rho^2}\,.$$

The coordinate transforms, as well as the change of variables (31), also act on the boundary conditions. In Fourier spectral space, with the superscripts 1, −1 and 0 for the upper ($z = 1$), lower ($z = -1$) and lateral ($r = 1$) part of the $(\rho - \zeta)$ domain, from Eq. (35) we have

$$\left(\alpha_3^{\mu} + \beta_3^{\mu}\frac{\mathrm{d}z}{\mathrm{d}\zeta}\partial_z\right)\tilde{\omega}_3(r, z = \mu; k) = \tilde{f}_3^{\mu}(r; k)\,, \quad \mu = -1, 1\,, \quad 0 \leqslant k \leqslant K\,,$$

$$\left(\alpha_3^0 + \beta_3^0\frac{m}{\rho} + \beta_3^0\frac{\mathrm{d}r}{\mathrm{d}\rho}\partial_r\right)\tilde{\omega}_3(r = 1, z; k) = \tilde{f}_3^0(z; k)\,, \quad 0 \leqslant k \leqslant K\,. \tag{A.2}$$

One can now proceed to the discretization of the (r, z) plane and look for the discretized form of the problem (A.1), (A.2). Due to the fact that $\tilde{\omega}_3$ and $r(\rho)$ are even in ρ, $\tilde{\omega}_3$ is even in r and so it is only necessary to consider the collocation points such as $r \geq 0$. Moreover, the pseudo-singularity of the Laplacian implies that no collocation point can occur at the z axis ($r = 0$). The classical Gauss–Lobatto mapping has to be restricted to

$$z_i = \cos\frac{\pi i}{I}, \quad 0 \leq i \leq I,$$
$$r_j = \cos\frac{\pi j}{J}, \quad 0 \leq j \leq J' = \frac{J-1}{2} \ (J \text{ odd}). \tag{A.3}$$

The collocation method consists of expressing all the derivatives as linear combinations of the values at the collocation points. In z, the usual approximations of the first or second order derivatives yield [14], e.g. for the first order,

$$\partial_z \tilde{\omega}_3(i, j; k) = \sum_{i'=0}^{I} d^z_{i,i'} \tilde{\omega}_3(i', j; k). \tag{A.4}$$

In the r direction one takes advantage of the parity of $\tilde{\omega}_3$ by writing

$$\partial_r \tilde{\omega}_3(i, j; k) = \sum_{j'=0}^{J'} (d^r_{j,j'} + d^r_{j,J-j'}) \tilde{\omega}_3(i, j'; k). \tag{A.5}$$

Such relations permit us first to express the boundary conditions (A.2); straightforward calculations yield equations expressing the boundary values as linear combinations of internal values:

$$\tilde{\omega}_3\left(\frac{I - \mu I}{2}, j; k\right) = \sum_{i'=1}^{I} \gamma^{\mu}_{i'}(k) \tilde{\omega}_3(i', j; k) + \gamma^{\mu}_0(j; k), \quad \mu = -1, 1,$$
$$\tilde{\omega}_3(i, 0; k) = \sum_{j'=1}^{J'} \gamma^0_{j'}(k) \tilde{\omega}_3(i, j'; k) + \gamma^0_0(i; k), \tag{A.6}$$

where the multiplicative coefficients depend on the parameters α_3 and β_3 of Eq. (A.2) and where the additive coefficients depend on the function f_3.

Then, the collocation method expresses that at each internal collocation point, Eq. (A.1) is exactly verified. Using the expressions (A.6), which permit us to take out the boundary values, for each harmonic k, one obtains the matrix equation

$$AU + UB - \sigma U = S. \tag{A.7}$$

The matrix U (dimension $I - 1, J'$) contains all the values of $\tilde{\omega}_3(k)$ at the internal collocation points; A (dimension $I - 1$, $I - 1$) and B (dimension J', J') are square matrices associated with the derivative operators in z and r, respectively. Let us notice that matrix A does not depend on the mode number k, in contrast to matrix B. Both of them are real, and so the real and imaginary parts of U are solved independently.

In order to solve Eq. (A.7) it is interesting to use the 'diagonalization method' (see e.g. [14]), especially for transient problems, when the solutions must be computed at each time step. Nevertheless, the derivative matrices usually exhibit real eigenvalues, because they are associated with the Laplacian operator. In Eq. (A.7), matrix B may exhibit complex eigenvalues, because it is associated with the operator $\partial_{\rho\rho} + (2m + 1)\partial_\rho/\rho$.

Let us suppose first that all the eigenvalues of the matrices A and B are real. With Λ_A and Λ_B the diagonal matrices of the eigenvalues, M_A and M_B the matrices of the eigenvectors, knowing that $\Lambda_A = M_A^{-1} A M_A$, $\Lambda_B = M_B^{-1} B M_B$, we obtain.

$$\Lambda_A U' + U' \Lambda_B - \sigma U' = S', \tag{A.8}$$

with $U' = M_A^{-1} U M_B$ and $S' = M_A^{-1} S M_B$.

This matrix equation yields a set of uncoupled scalar equations which permits the calculation of U'. Then, one can compute $U = M_A U' M_B^{-1}$.

Let us suppose now that two of the eigenvalues of B are conjugate complex, e.g. $\lambda_{j=1}$ and $\lambda_{j=2}$, as well as the two associated eigenvectors $V_{j=1}$ and $V_{j=2}$ of M_B. Introducing the following partition of Λ_B and M_B:

$$\Lambda_B = \begin{bmatrix} \Lambda_B^{(1)} & 0 \\ 0 & \Lambda_B^{(2)} \end{bmatrix}, \quad \Lambda_B^{(1)} = \begin{bmatrix} \lambda_1 & 0 \\ 0 & \bar{\lambda}_1 \end{bmatrix}, \quad M_B = [M_B^{(1)} \quad M_B^{(2)}], \quad M_B^{(1)} = [V_1 \quad \bar{V}_1], \tag{A.9}$$

one can easily demonstrate that the real matrices J_B and P_B,

$$J_B = \begin{bmatrix} J_B^{(1)} & 0 \\ 0 & \Lambda_B^{(2)} \end{bmatrix}, \quad J_B^{(1)} = \begin{bmatrix} \mathrm{Re}(\lambda_1) & -\mathrm{Im}(\lambda_1) \\ \mathrm{Im}(\lambda_1) & \mathrm{Re}(\lambda_1) \end{bmatrix},$$
$$P_B = [P_B^{(1)} \quad M_B^{(2)}], \quad P_B^{(1)} = [\mathrm{Re}(V_1) \quad -\mathrm{Im}(V_1)], \tag{A.10}$$

are such that

$$BP_B = P_B J_B . \tag{A.11}$$

Starting from the equality,

$$\begin{bmatrix} 1 & \mathrm{i} \\ 1 & -\mathrm{i} \end{bmatrix} \mathrm{J}_\mathrm{B}^{(1)} = \Lambda_\mathrm{B}^{(1)} \begin{bmatrix} 1 & \mathrm{i} \\ 1 & -\mathrm{i} \end{bmatrix}, \quad (\mathrm{i}^2 = -1), \tag{A.12}$$

and multiplying on the right the matrix equation,

$$BM_B = M_B \Lambda_B \tag{A.13}$$

by the complex matrix C such that,

$$C = \begin{bmatrix} C^{(1)} & 0 \\ 0 & I \end{bmatrix}, \quad C^{(1)} = \frac{1}{2} \begin{bmatrix} 1 & \mathrm{i} \\ 1 & -\mathrm{i} \end{bmatrix} \quad (\mathrm{I} \text{ is the identity matrix}), \tag{A.14}$$

one obtains the result (A.11).

Such an approach can be extended to more than one couple of conjugate eigenvalues; each couple has to be replaced by a real 2×2 matrix to constitute the matrix J_B, and the associated eigenvectors by their real and imaginary parts to constitute the matrix P_B. Now, following an approach similar to the classical one, one obtains

$$\Lambda_A U'' + U'' J_B - \sigma U'' = S'', \tag{A.15}$$

with $U'' = M_A^{-1} U P_B$ and $S'' = M_A^{-1} S P_B$.

Such a matrix equation can be easily solved because it yields a set of scalar equations, uncoupled or at most coupled two by two.

REMARK. In the general case, for which both A and B may have complex eigenvalues, a similar approach is still possible by introducing matrices J_A and P_A; then, the scalar equations are uncoupled, coupled two by two, three by three or at most four by four.

References

[1] G.J. Hirasaki and J.D. Hellums, A general formulation of the boundary conditions on the vector potential in three-dimensional hydrodynamics, Quart. Appl. Math. 26 (1968) 331.

[2] G.J. Hirasaki and J.D. Hellums, Boundary conditions on the vector and scalar potentials in viscous three-dimensional hydrodynamics, Quart. Appl. Math. 28 (1970) 293.

[3] S.M. Richardson and A.R.H. Cornish, Solution of three-dimensional incompressible flow problems, J. Fluid Mech. 82 (1977) 309.

[4] A. Bendali, J.M. Dominguez and S. Gallic, A variational approach for the vector potential formulation of the Stokes and Navier-Stokes problems in three dimensional domains, J. Math. Anal. 107 (1985) 537.
[5] A.K. Wong and J.A. Reizes, The vector potential in the numerical solution of three-dimensional fluid dynamics problems in multiply connected regions, J. Comput. Phys. 62 (1986) 124.
[6] L. Morino, Helmholtz decomposition revisited: vorticity generation and trailing edge condition, Comput. Mech. 1 (1986) 65.
[7] J.L. Achard et E. Canot, Formulation intégro-différentielle pour les écoulements transitoires d'un fluide isovolume et visqueux, J. Méc. Théor. Appl. 7 (1988) 645.
[8] C. Canuto, M.Y. Hussaini, A. Quarteroni and T.A. Zang, Spectral Methods in Fluid Dynamics (Springer, Berlin, 1988) 90.
[9] A.T. Patera and S.A. Orszag, instability of pipe flow, in: A.R. Bishop, D.K. Campbell and B. Nicolaenko, eds., Non Linear Problems: Present and Future (North-Holland, Amsterdam, 1982).
[10] J.P. Pulicani and J. Ouazzani, A Fourier-Chebyshev pseudospectral method for solving steady 3D Navier-Stokes and heat equation in cylindrical cavities, Comput. & Fluids 20 (1991) 93.
[11] S.A. Orszag, Fourier series on spheres, Mon. Weather Rev. 12 (1973) 224.
[12] L. Tuckerman, Divergence-free velocity fields in non periodic geometries, J. Comput. Phys. 80 (1989) 403.
[13] S. Bonazzola and J.A. Marck, Three-dimensional gas dynamics in a sphere, J. Comput. Phys. 87 (1990) 201.
[14] U. Ehrenstein and R. Peyret, A Chebyschev collocation method for the Navier-Stokes equations with application to double diffusive convection, Internat. J. Numer. Methods Fluids 9 (1989) 427.
[15] J.M. Vanel, R. Peyret and P. Bontoux, A pseudospectral solution of vorticity-stream function equations using the influence matrix technique, in: K.N. Morton and M.J. Baines, eds., Numerical Methods for Fluid Dynamics II (Clarendon Press, Oxford, 1986).
[16] H.K. Moffatt, Viscous and resistive eddies near a sharp angle, J. Fluid Mech. 18 (1964) 1.
[17] L. Kleiser and U. Schumann, Treatment of incompressibility and boundary conditions in 3-D numerical spectral simulations of plane channels flows, in: E.H. Hirschel, ed., Proc. 3rd GAMM Conf. Numerical Methods in Fluid Mechanics, Notes on Numerical Fluid Mechanics, Vol. 2 (Vieweg, Braunschweig, 1980) 165.
[18] D. Funaro and D. Gottlieb, A new method of imposing boundary conditions in pseudospectral approximations of hyperbolic equations, Math. Comp. 51 (1988) 599.
[19] R.D. Moser, P. Moin and A. Leonard, A spectral numerical method for the Navier-Stokes equations with applications to Taylor-Couette flow, J. Comput. Phys. 52 (1983) 524.
[20] J.D. Ramshaw, A method for enforcing the solenoidal condition on magnetic field in numerical calculations, J. Comput. Phys. 52 (1983) 592.
[21] F. Assous, P. Degond, E. Heintze, P.A. Raviart and J. Segre, On a finite element method for solving the three-dimensional Maxwell equations, Proc. Workshop, Semiconductuers et Dispositifs Hyperfréquences, ENS Cachan (1992) 45.
[22] R. Pasquetti, R. Peyret, J.M. Lacroix and R. Bwemba, Spectral method and vorticity-potential vector formulation for three-dimensional cylindrical convection 2nd Internat. Forum Proc., Expert Systems and Computer Simulation in Energy Engineering, Erlangen (1992) 8.2.
[23] G. Neumann, Three-dimensional numerical simulations of buoyancy driven convection in vertical cylinders heated from below, J. Fluid Mech. 214 (1990) 559.
[24] E. Crespo, P. Bontoux, C. Smutek, B. Roux, G. Hardin, R. Sani and F. Rosenberger, Three-dimensional simulations of convection regimes in cylindrical ampoules. Comparisons with theoretical analyses and experiments, Proc. 6th European Symp. on Material Sciences under microgravity conditions, Bordeaux, France (1986) 529.
[25] R. Pasquetti, R. Bwemba and J.M. Lacroix, Spectral calculations of cylindrical convection using the vorticity–potential vector formulation, Proc. Heat Transfer 92 Conf., Milan, Italy (1992) 255.
[26] R. Pasquetti, R. Bwemba and J.M. Lacroix, Convection cylindrique 3D par méthode spectrale et formulation tourbillon–potentiel vecteur, Proc. SFT 92 Annual Conf., Sophia Antipolis, France (1992) 203.